

A novel robust control for disturbed uncertain microbial fuel cell with noisy output

Li Fu^{1*}

¹ College of Information & Control Engineering, Jilin Institute of Chemical Technology, Jilin 132022, China,
Corresponding Author Email: lifu.jilin@gmail.com

<https://doi.org/10.14447/jnmes.v28i1.a08>.

ABSTRACT

Received: March 24, 2024

Accepted: October 10, 2024

Keywords:

Microbial Fuel Cell, Parametric Uncertainty, Disturbances, Noise, Nonlinear Model, Lyapunov Stability, Adaptive Control, Chebyshev Neural Network

Microbial fuel cell (MFC) is one of the most important renewable sources for energy supply and reduction of environmental pollution, which has affected by various adversities due to operating conditions. In this paper, there are several serious issues related to the stable operation of a microbial fuel cell that have considered in the design of the controller, including: 1- Nonlinear terms that are of hard type; 2- Uncertainty of the model which is of parametric type and includes changes in temperature, environment and concentration; 3- Disturbances into the system which are of both matched and unmatched types; 4- And noise on the fuel cell output which has different origins. Also, the nonlinear model of MFC has considered for a more accurate description of system dynamics. By using of output feedback, adaptive, and sliding mode methods, and developing an approximation based on chebyshev neural network, a novel robust hybrid technique has proposed for controlling MFC output voltage and power. Using chebyshev neural network which has a simple structure with a suitable computational volume, the uncertainties, disturbances and hard nonlinear terms have approximated, and the optimal weights of the approximation have obtained by designing adaptive laws. Also, the robust part of the controller eliminates the effects of estimation error and noise. The Lyapunov's theory has used to ensure the stability of the closed-loop system. Furthermore, simulation in MATLAB environment and making comparison with the recent three robust methods in a strong scenario shows the efficiency of the proposed control method.

1. INTRODUCTION

Energy as the driving force of productive activities is the basic foundation of economic and social activities of any country. Restrictions on fossil fuels and the prediction of rising prices, environmental problems and air pollution, global warming, population growth, and energy insecurity following political and economic crises require a move toward renewable energy. The energy part is responsible for the emission of two-thirds of greenhouse gases, and the development and expansion of renewable energy helps to achieve the goals of economic, social and environmental development, which are key factors in achieving sustainable development, so it is a shortcut in this area. Unlike fossil fuels, renewable energy is essentially environmentally friendly that is not finite that means has a long life and natural cycles and due to the abundance and proper geographical distribution, it has led to decentralization in energy production and can guarantee the continuity of energy consumption for future generations by overcoming the limitation of energy resources [1-4]. In general, the most important current drivers for the development of renewable energy are: 1- Reducing the severity of the effects of climate change; 2- Reducing local air pollution; 3- Energy security; 4- Reducing costs, job creation and local value; 5- Ability to develop in remote areas.

Among the types of energy available for renewable energy production, fuel cell is of great importance, because by

clearing and recycling waste, it can achieve the goals of providing sustainable energy and preventing the release of pollutants simultaneously [5-6]. In this technology, high efficiency electrical energy is produced by direct combination of fuel and oxidizer. The most important advantages of this technology are simple installation, modular structure, high efficiency, high power density and longevity, and it can be used in transportation, power plants, portable electronics and military industries [7-8]. Based on the type of electrolyte, the fuel cell is divided into PEMFC, AFC, PAFC, MFC, etc. In this study, a control method has been implemented on the microbial fuel cell (MFC). The MFC has the ability to use microorganisms to oxidize the substrate and generate electrical energy, making it as an attractive option for long-term electrical generation. This type of fuel cell uses inexpensive and long-lasting electrodes for efficient, stable and low-cost wastewater treatment, and in addition to reduce water pollution, uses wastewater and other waste as fuel in the anode chamber. MFC also has the ability to produce biohydrogen and is used as a biosensor [9-10].

To date, various control methods have been implemented on MFC. In [11-12] to achieve the constant output voltage, adaptive fuzzy and PID fuzzy methods are used, respectively. In [13], the model predictive control method is used to achieve a fast response, while disturbances in temperature and substrate concentration are considered. To cover the uncertainty effects in MFC, the adaptive backstepping control

method is presented in [14]. In [15] by linearizing the MFC model around the working point, the linear matrix inequality (LMI) method has been used to control this type of fuel cell. To date, the most complete MFC control works have been presented in [16-18]. In [16], Imani et al. by taking account the uncertainty effect without linearization, have used the adaptive sliding mode method to achieve a constant output voltage. Under the same conditions, Fu et al. have used the finite-time sliding mode method for achieving a constant voltage and uncertainty coverage [17]. Of course, the same authors in [18], in addition to seeing the uncertainty, have also considered the disturbance on the fuel cell and have used the robust fuzzy method to control the MFC. Despite the work done to date, there are still shortcomings in MFC control that need to be addressed.

In this study, several issues have been considered simultaneously. The first is the nonlinear model of a microbial fuel cell. In many of the designed control methods, nonlinear terms elimination or linearization occurs around the work point, which results in the loss of much of the microbial fuel cell information. Therefore, preventing this case is the first goal of this study in controller design. The second issue is the existence of uncertainty and disturbance in the MFC model. Despite of the extensive efforts to accurately describe the fuel cell system due to operating conditions, flow rate changes, temperature variations, and of course changes in substrate concentration, there will certainly be uncertainty and disturbance in the MFC model which must be considered to achieve a constant output voltage and optimum power. The third problem is related to the noise. In a fuel cell environment and under different operating conditions, there are different types of noise and electrochemical interference that affect the output signal and the designed controller must be robust to its effects. Due to the fact that practical measurements are not perfect, the noise on the output signal can be caused by this fact or it can be caused by electrochemical processes, gas emission, mass transfer, etc. Each of these phenomena is a kind of reminder that there must be noise on the fuel cell output signal and its effects must be covered in some way. Therefore, achieving the optimal performance of MFC in delivering optimal power and constant output voltage despite the mentioned problems are the most important motivations of the study.

For this purpose, a new robust method is designed for optimal MFC control in this paper. The proposed method is based on neural network, adaptive, output feedback and sliding model methods and offers the following functions: 1- The control-oriented model of MFC is presented in which, in addition to covering nonlinear effects, an uncertainty term is also considered; 2- The neural network part in the controller is responsible for approximating all uncertainty terms, disturbances and hard nonlinearities in the model; 3- The adaptive method is used to obtain the optimal weights of the neural network; 4- To design a robust controller, system outputs are used rather than states, on which noise is mounted. The effects of estimation error and noise are also covered by the sliding mode method. It should be noted that the control signal enters only one of the states, so there is a double limitation in this regard, because a control signal should be able to stabilize all states of the system. In the proposed sliding mode method, the hyperbolic tangent function is used instead of the sign function to obtain the control signal and to avoid the fluctuations.

Therefore, the most important innovation of this paper is to present a new combined approach based on adaptive neural network and twisting sliding mode methods. The stability of the closed-loop system under the controller has already been shown, while in this study we have no knowledge on the upper bound of uncertainty and disturbance. The same is true about noise, nevertheless that we do not even know the nature of noise.

Accordingly, this article is organized as follows. In the second part, the nonlinear model of the microbial fuel cell is fully described. In the third section, with a review of the chebyshev neural network, the proposed control method is comprehensively explained. The fourth part is related to simulations and in this part, a scenario is considered to show the capability of the proposed method. Finally, the conclusion section is given at the end of the article.

2. NONLINEAR MFC MODEL with SINGLE CHAMBER

In this section, the nonlinear model of MFC is presented and described. The schematic of the corresponding model is shown in Figure 1.

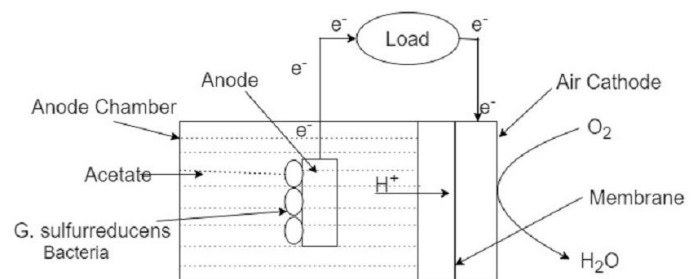
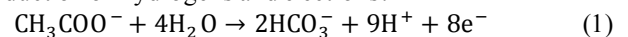


Figure 1. Single Chamber MFC with Membrane

In the anode chamber, the following reaction occurs between microorganisms and substrate, leading to the production of hydrogens and electrons.



The structure of a single-chamber MFC is such that electrons are transferred to the cathode through mediators, anodes, and external electrical circuits, and proteins are transferred to the cathode via a cation membrane. Through the following reaction between electrons and hydrogen with oxygen (air) injected on the cathode side, the MFC output is the same as ordinary water.



It should be noted that in the model under study, acetate is the substrate and *G. sulfurreducens* is the bacterium, and the first mathematical model was developed in [19] for it. Given that microorganisms are present in the anode chamber due to biomass, if substrate feeding occurs at the rate of Q_a , we have C_s and X as concentrations of substrate and biomass, respectively.

$$\frac{dC_s}{dt} = q_{max} \frac{C_s}{k_s + C_s} X + D(S_o - C_s), \quad (3)$$

$$\frac{dX}{dt} = \mu_{max} \frac{C_s}{k_s + C_s} X - k_d X - DX, \quad (4)$$

Where μ_{max} , q_{max} state the maximum rate of substrate utilization, and the maximum growth rate respectively, S_o , k_d and k_s specify the influent substrate concentration, biomass decay co-efficient and half saturation constant respectively, D

states the dilution rate defined as a ratio of the flow rate and the chamber volume. The reciprocal of biomass yield coefficient, k_1 equals to $\frac{\mu_{\max}}{\mu_{\max}}$.

Also, the mass equilibria related to H^+ and HCO_3^- are as follows:

$$\frac{dH^+}{dt} = 9 \frac{dC_s}{dt}, \quad (5)$$

$$\frac{dHCO_3^-}{dt} = 2 \frac{dC_s}{dt}, \quad (6)$$

Considering the concentrations of $[C_s, X, H^+, HCO_3^-]$ as state variables $[x_1, x_2, x_3, x_4]$, dilution rate D as control input u and μ_{\max} as θ_1^{-1} , the state space equations related to MFC are as follows:

$$\dot{x}_1 = \theta_1^{-1} k_1 r(x_1) x_2 + u(S_0 - x_1), \quad (7)$$

$$\dot{x}_2 = (\theta_1^{-1} r(x_1) x_2 - k_d - u) x_2 \quad (8)$$

$$\dot{x}_3 = 2\dot{x}_1, \dot{x}_4 = 9\dot{x}_1, \quad (9)$$

In the above model $r(x_1) = \frac{x_1}{k_s + x_1}$, and as it turns out, the states x_3 and x_4 are coefficients of x_1 .

3. CONTROLLER DESIGN

This section describes the proposed controller structure. There are several issues in the microbial fuel cell model under study. The existence of parametric uncertainty is the first problem in controller design. As mentioned in the introduction, due to changes in environmental conditions and other factors, there is uncertainty in the MFC model and its effects should be considered in the controller design. The second problem is the existence of hard nonlinear terms. To avoid the disadvantages of linearization, which includes limiting the functional range and, of course, eliminating information, the effects of all nonlinear factors are considered in the controller design. The next challenge in designing a controller is to deal with disturbances in the system. Two types of disturbances enter the two main states of the fuel cell system and due to their destructive effects, it is necessary to consider them. Finally, another challenge is the presence of noise in the output. In controller design studies so far, the effect of this component isn't considered while it has a significant impact on the output of the fuel cell system. It should be noted that different noises are mounted on the outputs of the fuel cell system, which exacerbates the controller design problems.

Both the uncertainty and the disturbance intervals in the fuel cell system are finite, but their upper limits are not known to us. Also, due to the structure of the MFC, the control operation should be performed only by designing one control signal. In this paper, a combination of sliding mode, adaptive and chebyshev neural network methods have been used to cover all the mentioned factors in addition to reaching the desired working point for the fuel cell. The schematic of the proposed control method is shown in Figure 2. Neural network method has been used for uncertainty and nonlinear terms approximation. To cover the effects of disturbance and noise derivation and also to ensure the stability of the closed loop, the robust sliding mode method has been used. The adaptive method has also been used to obtain the optimal fuzzy approximating weights and gains of the sliding mode method as well as the upper boundaries of uncertainty and disturbance. After reviewing the chebyshev neural network, we will describe the different design steps of this controller.

3.1 Approximation using chebyshev neural network

Inspired by the function of the biological neural system, the artificial neural network provides new computational methods for learning, data storage, and output prediction of complex systems, and has been used as a powerful tool for identification and approximation in this study. Various structures have been used as artificial neural networks, including 1- multilayer perceptron (MLP); 2- chebyshev neural networks (CNNs); 3- radial basis function network (RBFN); 4- recurrent neural networks and so on. In the proposed control method, CNN method is used for identification and approximation, due to less complexity in structure modeling, it is very efficient for calculation and has a high convergence speed, and it is very easy to implement compared to multilayer neural networks.

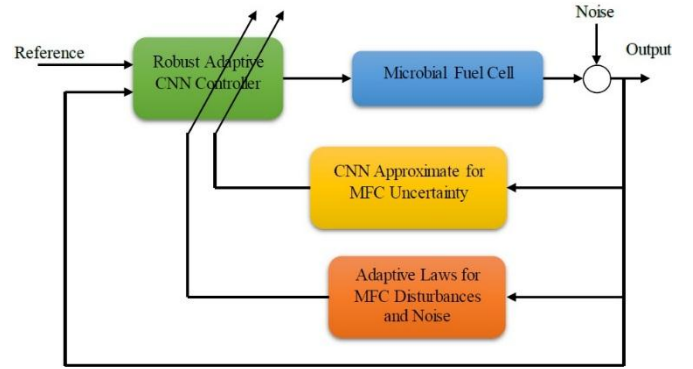


Figure 2. Block diagram of the MFC system with proposed controller

The single-layer structure of CNNs provides a functional link network based on chebyshev polynomials. These polynomials are the solution to the differential equations of chebyshev and are obtained from the following recursive equation.

$$T_{i+1}(x) = 2xT_i(x) - T_{i-1}(x), T_0(x) = 1 \quad (10)$$

Where, $T_1(x)$ specify Chebyshev polynomials, i indicates the order of polynomials taken and x states a scalar number. The different selections of $T_1(x)$ are x & $2x$.

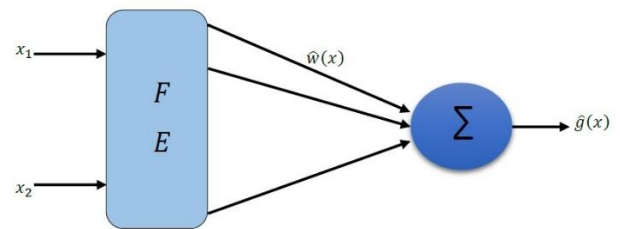


Figure 3. Chebyshev Neural Network [19]

The output of the single layer neural network is obtained by the following equation:

$$\hat{g}(x) = \hat{w}^T \phi \quad (11)$$

Where w and ϕ state the weights and the basis function of neural network, respectively. According to the approximation property of CNN, there are ideal weights w , such that the function $g(x)$ for the approximation can be signified as

$$g(x) = w^T \phi + \varepsilon \quad (12)$$

Where, ε states the CNN functional reconstruction error vector and $\|\varepsilon\| \leq \varepsilon_N$ is bounded. Approximation of complex nonlinear systems becomes easier when CNN is a single-layer neural network.

3.2 Proposed control method

The equations of the microbial fuel cell system are considered as follows:

$$\dot{x}_1 = -\theta^{-1}y^{-1}\frac{x_1}{k_s + x_1}x_2 + u(c_{s_0} - x_1) + d_1(t) \quad (13)$$

$$\dot{x}_2 = \left(\theta^{-1}\frac{x_1}{k_s + x_1} - k_d - u\right)x_2 + d_2(t)$$

$$y = \begin{bmatrix} 1 & 0 \\ 0 & 1 \end{bmatrix} \begin{bmatrix} x_1 \\ x_2 \end{bmatrix} + \begin{bmatrix} n_1(t) \\ n_2(t) \end{bmatrix} \rightarrow \begin{cases} y_1 = x_1 + n_1(t) \\ y_2 = x_2 + n_2(t) \end{cases}$$

Where $n_1(t)$ and $n_2(t)$ are the system output noises. In the above equations, θ can change under different conditions which is considered as an uncertainty interval in this study. The coefficient $\frac{x_1}{k_s + x_1}$ appears as a nonlinear term in both states. The only control signal available to control both x_1 and x_2 is u , ie there is only one signal to control the two outputs and reach the two desired values. The $d_1(t)$ and $d_2(t)$ are two different disturbances that negatively affect the x_1 and x_2 states. If we consider the system outputs y_1 and y_2 , we see that two different noises $n_1(t)$ and $n_2(t)$ enter the two outputs of the fuel cell system, and of course these noises are also different from each other. The simultaneous coverage of the effects of 1- uncertainty 2- nonlinear terms 3- various disturbances 4- different noises are the aims of this study and this should be done only by one control signal.

Now we define the error as follows:

$$e_1 = y_1 - y_{1d} \quad (14)$$

$$e_2 = y_2 - y_{2d}$$

The error equation indicates that the first output, y_1 must follow the desired value of y_{1d} , and the second output, y_2 must follow the desired value of y_{2d} .

Derived from the error, the dynamic equations of the error are obtained as follows:

$$\dot{e}_1 = \dot{x}_1 + \dot{n}_1(t) - \dot{y}_{1d} \quad (15)$$

$$= -\theta^{-1}y^{-1}\frac{x_1}{k_s + x_1}x_2$$

$$+ u(c_{s_0} - x_1) + d_1(t) + \dot{n}_1(t)$$

$$- \dot{y}_{1d}$$

$$\dot{e}_2 = \dot{x}_2 + \dot{n}_2(t) - \dot{y}_{2d}$$

$$= \left(\theta^{-1}\frac{x_1}{k_s + x_1} - k_d - u\right)x_2$$

$$+ d_2(t) + \dot{n}_2(t) - \dot{y}_{2d}$$

In the resulting error dynamics, all elements of uncertainty, disturbance, hard nonlinear terms, noise and its derivatives are presented simultaneously.

Because the control signal u exists only in one of the states, and to overcome this limitation, we have defined it as follows:

$$u = u_1 + u_2 \quad (16)$$

Where u_1 will be used to control the first state and u_2 will be used to control the second state.

By placing the control signal, the error dynamics is obtained as follows:

$$\dot{e}_1 = f_1(t, y, u) + c_{s_0}u_1 + \delta_1(t) \quad (17)$$

$$\dot{e}_2 = f_2(t, y, u) - u_2 + \delta_2(t)$$

And the definitions for f_1 , f_2 , δ_1 and δ_2 are as follows:

$$f_1(t, y, u) = -\theta^{-1}y^{-1}\frac{y_1 - n_1(t)}{k_s + y_1 - n_1(t)}(y_2 - n_2(t)) - u(y_1 - n_1(t) + c_{s_0}u_2 - \dot{y}_{1d}) \quad (18)$$

$$f_2(t, y, u) = \theta^{-1}\frac{y_1 - n_1(t)}{k_s + y_1 - n_1(t)}(y_2 - n_2(t)) - k_d(y_2 - n_2(t)) - (y_1 - n_1(t) - 1)u - u_1 - \dot{y}_{2d}$$

$$\delta_1(t) = d_1(t) + \dot{n}_1(t) \quad (19)$$

$$\delta_2(t) = d_2(t) + \dot{n}_2(t)$$

As it turns out, f_1 and f_2 , in addition to uncertainty, the nonlinear terms and the noise include the interactions resulting from the new definition of the control signal in equation (16).

To ensure the stability of the system and at the same time achieve the control objectives, the following Lyapunov function is nominated.

$$V = \frac{1}{2}e_1^2 + \frac{1}{2}e_2^2 + \frac{1}{2\lambda_1}\tilde{W}_1^T\tilde{W}_1 + \frac{1}{2\lambda_2}\tilde{W}_2^T\tilde{W}_2 + \frac{1}{2\lambda_3}\tilde{B}_1^2 + \frac{1}{2\lambda_4}\tilde{B}_2^2 \quad (20)$$

where

$$\tilde{W}_1 = W_1 - \hat{W}_1$$

$$\tilde{W}_2 = W_2 - \hat{W}_2$$

$$\tilde{B}_1 = B_1 - \hat{B}_1$$

$$\tilde{B}_2 = B_2 - \hat{B}_2$$

If W_1 and W_2 represent the actual weights f_1 and f_2 , \hat{W}_1 and \hat{W}_2 represent the estimated weights obtained from the chebyshev neural network to estimate f_1 and f_2 , and it is necessary to consider the difference between the actual and the estimated values in Lyapunov's function to ensure stability. Also, if B_1 and B_2 are the upper boundaries for δ_1 and δ_2 , \hat{B}_1 and \hat{B}_2 are the estimates of these boundaries and the magnitude of the error between the real and estimated boundaries are considered in the Lyapunov function with the terms \tilde{B}_1 and \tilde{B}_2 . The λ_3 and λ_4 also represent adaptive adjustment parameters.

The derivative of the Lyapunov function is obtained

$$\dot{V} = e_1\dot{e}_1 + e_2\dot{e}_2 - \frac{1}{\lambda_1}\tilde{W}_1^T\dot{\tilde{W}}_1 - \frac{1}{\lambda_2}\tilde{W}_2^T\dot{\tilde{W}}_2 - \frac{1}{\lambda_3}\tilde{B}_1\dot{\tilde{B}}_1 - \frac{1}{\lambda_4}\tilde{B}_2\dot{\tilde{B}}_2 = e_1(f_1(t, y, u) + c_{s_0}u_1 + \delta_1(t)) + e_2(f_2(t, y, u) - u_2 + \delta_2(t)) - \frac{1}{\lambda_1}\tilde{W}_1^T\dot{\tilde{W}}_1 - \frac{1}{\lambda_2}\tilde{W}_2^T\dot{\tilde{W}}_2 - \frac{1}{\lambda_3}\tilde{B}_1\dot{\tilde{B}}_1 - \frac{1}{\lambda_4}\tilde{B}_2\dot{\tilde{B}}_2 \quad (21)$$

$$+ \frac{1}{\lambda_3}\tilde{B}_1\dot{\tilde{B}}_1 - \frac{1}{\lambda_4}\tilde{B}_2\dot{\tilde{B}}_2 = e_1(f_1(t, y, u) + c_{s_0}u_1 + \delta_1(t)) + e_2(f_2(t, y, u) - u_2 + \delta_2(t)) - \frac{1}{\lambda_1}\tilde{W}_1^T\dot{\tilde{W}}_1 - \frac{1}{\lambda_2}\tilde{W}_2^T\dot{\tilde{W}}_2 - \frac{1}{\lambda_3}\tilde{B}_1\dot{\tilde{B}}_1 - \frac{1}{\lambda_4}\tilde{B}_2\dot{\tilde{B}}_2$$

By selecting u_1 and u_2 as follows:

$$u_1 = \frac{1}{c_{s_0}}(-\tilde{W}_1^T\varphi_1(y) - \hat{B}_1\tanh\left(\frac{e_1}{\eta_1}\right) - k_1\tanh(e_1)) \quad (22)$$

$$u_2 = \tilde{W}_2^T\varphi_2(y) + \hat{B}_2\tanh\left(\frac{e_2}{\eta_2}\right) + k_2\tanh(e_2)$$

In u_1 , the expression $\tilde{W}_1^T\varphi_1(y)$ which is obtained by the neural network method, is used to cover the effects of f_1 . The δ_1 is covered by the expressions $-\hat{B}_1\tanh\left(\frac{e_1}{\eta_1}\right)$ and the expression $-k_1\tanh(e_1)$ is to ensure stability in the presence of disturbance. How to select expressions in u_2 is similar to u_1 . It should be noted that due to the use of tangent functions instead of sign, the obtained control signals are smooth. By placing in (21), it is obtained:

$$\begin{aligned} \dot{V} = e_1 & \left(f_1(t, y, u) - \widehat{W}_1^T \varphi_1(y) + \delta_1(t) \right. \\ & - \widehat{B}_1 \tanh\left(\frac{e_1}{\eta_1}\right) - k_1 \tanh(e_1) \Big) \\ & + e_2 \left(f_2(t, y, u) - \widehat{W}_2^T \varphi_2(y) \right. \\ & + \delta_2(t) - \widehat{B}_2 \tanh\left(\frac{e_2}{\eta_2}\right) \\ & - k_2 \tanh(e_2) \Big) - \frac{1}{\lambda_1} \widehat{W}_1^T \dot{\widehat{W}}_1 \\ & - \frac{1}{\lambda_2} \widehat{W}_2^T \dot{\widehat{W}}_2 - \frac{1}{\lambda_3} \widehat{B}_1 \dot{\widehat{B}}_1 \\ & - \frac{1}{\lambda_4} \widehat{B}_2 \dot{\widehat{B}}_2 \end{aligned} \quad (23)$$

By mathematical simplification, it is obtained

$$\begin{aligned} \dot{V} = e_1 & \left(W_1^T \varphi_1(y) + \varepsilon_1 - \widehat{W}_1^T \varphi_1(y) + \delta_1(t) \right. \\ & - \widehat{B}_1 \tanh\left(\frac{e_1}{\eta_1}\right) - k_1 \tanh(e_1) \Big) \\ & + e_2 \left(W_2^T \varphi_2(y) + \varepsilon_2 \right. \\ & - \widehat{W}_2^T \varphi_2(y) + \delta_2(t) \\ & - \widehat{B}_2 \tanh\left(\frac{e_2}{\eta_2}\right) - k_2 \tanh(e_2) \Big) \\ & - \frac{1}{\lambda_1} \widehat{W}_1^T \dot{\widehat{W}}_1 - \frac{1}{\lambda_2} \widehat{W}_2^T \dot{\widehat{W}}_2 \\ & - \frac{1}{\lambda_3} \widehat{B}_1 \dot{\widehat{B}}_1 - \frac{1}{\lambda_4} \widehat{B}_2 \dot{\widehat{B}}_2 \end{aligned} \quad (24)$$

By placing f_1 and f_2 based on the chebyshev neural network

$$\begin{aligned} \dot{V} = e_1 & \widehat{W}_1^T \varphi_1(y) + e_1 \varepsilon_1 + e_1 \delta_1(t) \\ & - \widehat{B}_1 e_1 \tanh\left(\frac{e_1}{\eta_1}\right) \\ & - k_1 e_1 \tanh(e_1) + e_2 \widehat{W}_2^T \varphi_2(y) \\ & + e_2 \varepsilon_2 + e_2 \delta_2(t) \\ & - \widehat{B}_2 e_2 \tanh\left(\frac{e_2}{\eta_2}\right) \\ & - k_2 e_2 \tanh(e_2) - \frac{1}{\lambda_1} \widehat{W}_1^T \dot{\widehat{W}}_1 \\ & - \frac{1}{\lambda_2} \widehat{W}_2^T \dot{\widehat{W}}_2 - \frac{1}{\lambda_3} \widehat{B}_1 \dot{\widehat{B}}_1 \\ & - \frac{1}{\lambda_4} \widehat{B}_2 \dot{\widehat{B}}_2 \end{aligned} \quad (25)$$

Given the above equation and to eliminate the effects of the chebyshev estimation error, the adaptive rules for \widehat{W}_1 and \widehat{W}_2 are obtained as follows:

$$\dot{\widehat{W}}_1 = \lambda_1 e_1 \varphi_1(y) \quad (26)$$

$$\dot{\widehat{W}}_2 = \lambda_2 e_2 \varphi_2(y)$$

By placing adaptive laws (26) in (25), it is obtained

$$\begin{aligned} \dot{V} = & -k_1 e_1 \tanh(e_1) - k_2 e_2 \tanh(e_2) + e_1 \varepsilon_1 \\ & + e_2 \varepsilon_2 + e_1 \delta_1(t) \\ & - \widehat{B}_1 e_1 \tanh\left(\frac{e_1}{\eta_1}\right) + e_2 \delta_2(t) \\ & - \widehat{B}_2 e_2 \tanh\left(\frac{e_2}{\eta_2}\right) - \frac{1}{\lambda_3} \widehat{B}_1 \dot{\widehat{B}}_1 \\ & - \frac{1}{\lambda_4} \widehat{B}_2 \dot{\widehat{B}}_2 \end{aligned} \quad (27)$$

By simplifying (16) mathematically and placing the above boundaries for $\delta_1(t)$ and $\delta_2(t)$

$$\dot{V} \leq -k_1 e_1 \tanh(e_1) - k_2 e_2 \tanh(e_2) + e_1 \varepsilon_1 \quad (28)$$

$$\begin{aligned} & + e_2 \varepsilon_2 + |e_1| B_1 \\ & - B_1 e_1 \tanh\left(\frac{e_1}{\eta_1}\right) \\ & + \widehat{B}_1 e_1 \tanh\left(\frac{e_1}{\eta_1}\right) + |e_2| B_2 \\ & - B_2 e_2 \tanh\left(\frac{e_2}{\eta_2}\right) \\ & + \widehat{B}_2 e_2 \tanh\left(\frac{e_2}{\eta_2}\right) - \frac{1}{\lambda_3} \widehat{B}_1 \dot{\widehat{B}}_1 \\ & - \frac{1}{\lambda_4} \widehat{B}_2 \dot{\widehat{B}}_2 \end{aligned}$$

$$\begin{aligned} \dot{V} \leq & -k_1 e_1 \tanh(e_1) - k_2 e_2 \tanh(e_2) + e_1 \varepsilon_1 + \\ & e_2 \varepsilon_2 + \left(|e_1| - e_1 \tanh\left(\frac{e_1}{\eta_1}\right) \right) B_1 + \left(|e_2| - \right. \\ & \left. e_2 \tanh\left(\frac{e_2}{\eta_2}\right) \right) B_2 + \widehat{B}_1 \left(e_1 \tanh\left(\frac{e_1}{\eta_1}\right) - \frac{1}{\lambda_3} \dot{\widehat{B}}_1 \right) + \\ & \widehat{B}_2 \left(e_2 \tanh\left(\frac{e_2}{\eta_2}\right) - \frac{1}{\lambda_4} \dot{\widehat{B}}_2 \right) \end{aligned} \quad (29)$$

To eliminate the effects of \widehat{B}_1 and \widehat{B}_2 , it is necessary to specify the adaptive rules for estimating \widehat{B}_1 to \widehat{B}_2 as follows:

$$\dot{\widehat{B}}_1 = \lambda_3 e_1 \tanh\left(\frac{e_1}{\eta_1}\right) \quad (30)$$

$$\dot{\widehat{B}}_2 = \lambda_4 e_2 \tanh\left(\frac{e_2}{\eta_2}\right)$$

These equations eliminate the effects of noise and disturbance.

By placing the adaptive rules (30) in (29) and also considering the mathematical relation $0 \leq |x| - x \tanh\left(\frac{x}{\mu}\right) \leq 0.2785\mu$ from the reference [23], it is obtained:

$$\begin{aligned} \dot{V} \leq & -k_1 e_1 \tanh(e_1) - k_2 e_2 \tanh(e_2) + e_1 \varepsilon_1 \\ & + e_2 \varepsilon_2 + 0.2785 \eta_1 B_1 \\ & + 0.2785 \eta_2 B_2 \end{aligned} \quad (31)$$

By defining σ as follows:

$$\sigma = e_1 \varepsilon_1 + e_2 \varepsilon_2 + 0.2785 \eta_1 B_1 + 0.2785 \eta_2 B_2 \quad (32)$$

Equation (31) is rewritten as follows:

$$\dot{V} \leq -k_1 e_1 \tanh(e_1) - k_2 e_2 \tanh(e_2) + \sigma \quad (33)$$

Let $k = \min(k_1, k_2)$, given that the approximation error of chebyshev neural network and $\sigma > 0$ are bounded, then equation (33) can be modified as

$$\dot{V} \leq -k(e_1 \tanh(e_1) + e_2 \tanh(e_2)) + \sigma \quad (34)$$

By integrating the equation on the region $\xi \in [0, T]$

$$\begin{aligned} V(T) - V(0) \leq & -k \int_0^T (e_1 \tanh(e_1) \\ & + e_2 \tanh(e_2)) d\xi + \int_0^T \sigma d\xi \end{aligned} \quad (35)$$

Considering $V(T) \geq 0$ and by applying the control signal (16) as well as adaptive rules (26) and (30), closed-loop system is stable and ultimately bounded which is in-line with tracking error.

$$\begin{aligned} \int_0^T (e_1 \tanh(e_1) + e_2 \tanh(e_2)) d\xi \\ \leq \frac{1}{k} V(0) + \frac{1}{k} \int_0^T \sigma d\xi \end{aligned} \quad (36)$$

Therefore, without knowledge about the uncertainty range, without knowledge of the noise type entering the system and the disturbance bound, and even without knowledge about the

noise and nonlinear effects, and with only one control signal, we covered all our control demands, and we showed that under the proposed method, the closed-loop system is stable and the error remains in the boundary range.

4. SIMULATION RESULTS

In this section, the results obtained through simulation in MATLAB environment reviewed and are evaluated. The hardware used for simulation in MATLAB 2018a environment is as follows: Intel Core i7-10750H, 16GB DDR4 RAM, 512GB SSD, NVIDIA GeForce RTX 2060 6GB GDDR6.

The nominal values of the fuel cell parameters are given in Table 1.

Table 1. Values of Parameters and Constants

Symbol	Typical Value	Unit
k_1	0.09	—
X_0	1.5	mg L ⁻¹
$\mu_{max}(\theta^{-1})$	0.4	day ⁻¹
q_{max}	3.6	day ⁻¹
k_d	0.084	d ⁻¹
k_s	32.4	mg L ⁻¹
S_0	60	mg L ⁻¹
E_{oa}	0.187	V
E_{oc}	1.229	V
E_{La}	0.15	V
E_{Lc}	1.1019	V
R	08.311446	J. K ⁻¹ .mol ⁻¹
T	298.15	K
F	96485	s.A.mol ⁻¹
n_1	8	—
n_2	4	—

The proposed controller parameters used in this study are as follows:

$$k_1 = 20, k_2 = 1, \lambda_1 = 1 \times 10^{-2}, \lambda_2 = 1 \times 10^{-2}, \quad (37)$$

And for the part of chebyshev neural network:

$$k = 2, \lambda = 1 \times 10^{-5} \quad (38)$$

To more accurately evaluate the capability of the proposed method, the scenario considered for the simulation is as follows:

1- Noise enters the system with the following equation:

$$n(t) = 0.01\varepsilon(t) \quad (39)$$

In the above relation, ε is Gaussian white noise.

2- Parametric uncertainty is considered as follows in the simulation

$$\begin{cases} \theta^{-1} = 0.4 & \text{if } t < 40 \\ \theta^{-1} = 0.38 & \text{if } t \geq 40 \end{cases} \quad (40)$$

3- Disturbance is also embedded in this scenario with the following criteria

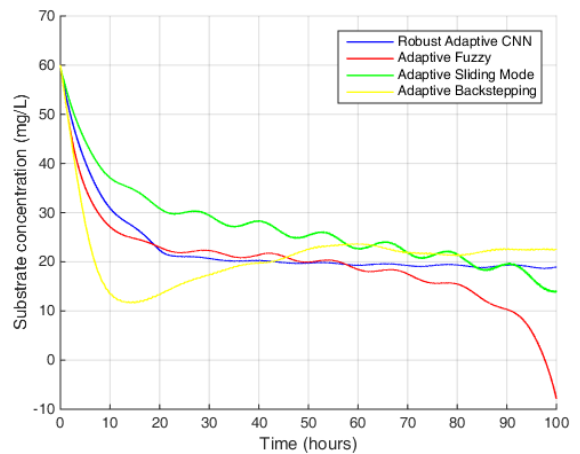
$$\begin{aligned} d_1(t) &= 0.02 \sin(0.3t) \\ d_2(t) &= 0.03 \cos(0.5t) \end{aligned} \quad (41)$$

The disturbance covers all changes related to load, temperature and ambient concentration. Therefore, all three adverse factors affecting the dynamics of the fuel cell system are considered in this scenario, and this state indicates the most severe and worst working conditions for fuel cell operation and the best way for testing the capability of the proposed controller.

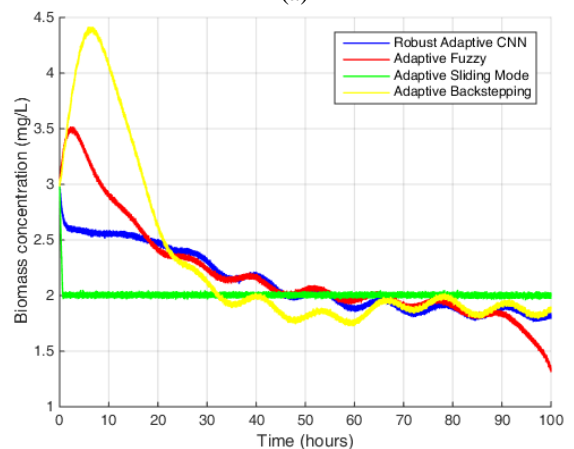
Also, for better evaluation, the results obtained from the implementation of the proposed control method are compared with adaptive fuzzy, adaptive sliding mode and adaptive backstepping control methods [16, 18, and 24]. Now the results are fully described.

Figure 4(a) shows the obtained substrate concentration. As it turns out, using the proposed CNN-based output feedback controller, the concentration is regulated accurately, while the adaptive fuzzy method is not able to stabilize the state and the substrate concentration at all. The adaptive sliding mode method shows almost the same behavior as the fuzzy method and only the adaptive backstepping method is able to regulate and stabilize the substrate concentration to some extent. Of course, it should be noted that in the backstepping method, the concentration level is experienced undershoot before reaching the final value, also there is an error between the final value and the desired value. So in the simulation scenario, in the first state, the desired operating point is followed only by the proposed control method, and other methods are not able to perform this regulation and stabilization of the system.

Figure 4(b) shows the results obtained for biomass concentrations. In this state, the adaptive sliding mode method is well able to regulate, but its drawback is the instability of the first state. The result obtained from the adaptive fuzzy method is unstable like the first state, but the adaptive backstepping and the proposed methods have been able to stabilize and regulate despite of the uncertainty, disturbance and noise. However, there is a small error of a few hundredths on the results obtained, which can be neglected due to the intensity and severity of the undesirable elements entering the system.



(a)



(b)

Figure 4. (a) Performance of substrate concentration (b) Performance of biomass concentration

The control signals obtained from the four methods are shown in Figure 5. As stated in the previous figure, the adaptive sliding mode and adaptive fuzzy methods are not able to stabilize the substrate and biomass concentrations, and this defect is evident from the control signal. Because the control signals obtained from these two methods give negative values, these values lead to instability of states under these two methods. Both signals from the proposed CNN-based feedback and the backstepping methods guarantee system stability, although the first state exhibits better transient and steady state behavior under the proposed method.

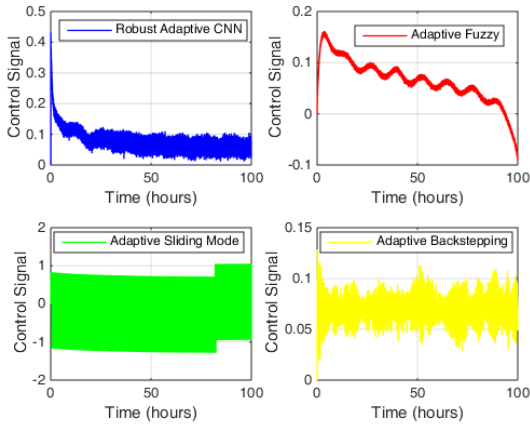
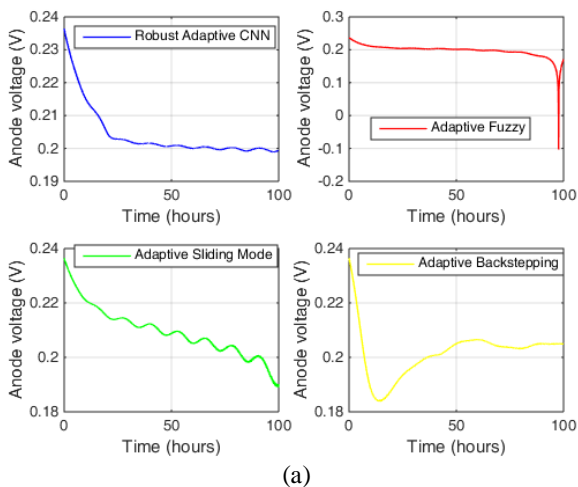


Figure 5. Control Signal

The results for the anode, cathode and MFC output voltages are shown in Figure 6. Carefully in these figures it can be seen that the obtained voltages are unacceptable and non-uniform for adaptive fuzzy and adaptive sliding mode controllers due to system instability, while the adaptive backstepping and the proposed methods provide acceptable values and uniformity for anode, cathode and MFC voltages. By carefully comparing of the results obtained for these two last methods, the superiority of the results obtained under the innovative method is clear in terms of permanent and transient response, because of the smoother behavior, without overshoot and undershoot, with better uniformity and of course higher output voltage than the adaptive backstepping method.



(a)

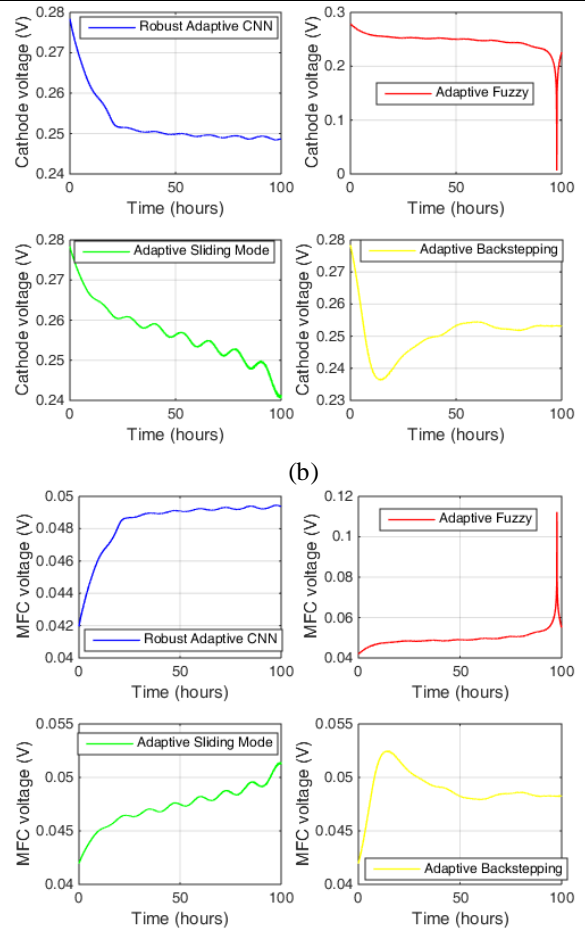


Figure 6. (a) Anode voltages of single chamber MFC (b) Cathode voltages of single chamber MFC (c) Voltages of single chamber MFC

The current obtained for MFC under different control methods is shown in Figure 7 (a). The interpretations given for the MFC voltage in the previous figure are the same for the MFC current, meaning that the adaptive fuzzy and adaptive sliding mode methods are not able to provide an acceptable current from the MFC, and the currents obtained from the two adaptive backstepping and the proposed methods follow the same voltage behavior, i.e. smoother behavior, without overshoot and undershoot, and better uniformity is obtained under the proposed method.

The MFC output power under the studied control methods is shown in Figure 7 (b). Considering the output current and voltage obtained in the adaptive fuzzy and adaptive sliding mode methods, the instability of the MFC output power under these two methods is obvious, as shown in Figure 7 (b). As Figures 6 and 7 (a), the two adaptive backstepping and the innovative methods provide acceptable output power and of course, like the results for voltage and current, the output power under the proposed method is smoother with better uniformity, without overshoot and undershoot, and in general has a better transient and steady state behavior than the backstepping method. As can be seen from Figure 7 (b), under the backstepping method, the MFC output power experiences a large overshoot and then reaches its steady state.

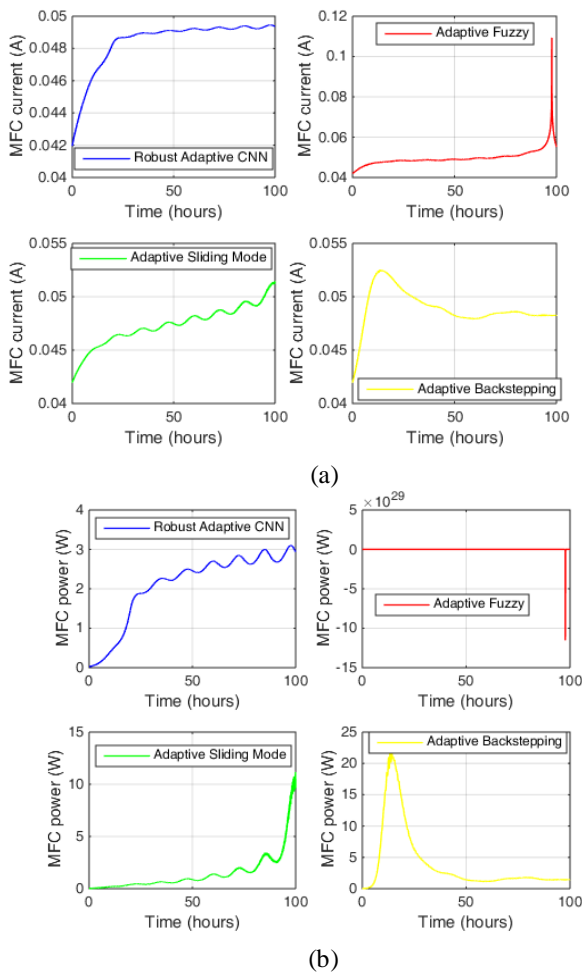


Figure 7. (a) Current of single chamber MFC (b) Output power of single chamber MFC

For a more accurate comparison, the error values of ISE, IAE, and ITAE for the two states of biomass and substrate concentrations are given in Table 2. As it is known, for the first state, better results are obtained under the innovative method for these three error definitions, and for the biomass concentration, the results obtained are better under the adaptive backstepping method. However, due to the small difference between the results obtained from the backstepping method and the proposed method, this advantage is negligible.

Table 2. The error comparison in the simulation scenario

Controller	State	ISE	IAE	ITAE
Robust Adaptive CNN	Substrate concentration (mg/L)	0.001	0.001	0.1
	Biomass concentration (mg/L)	3.35e-5	1.82e-4	0.01
Adaptive Fuzzy	Substrate concentration (mg/L)	unstable		
	Biomass concentration (mg/L)			
Adaptive Sliding Mode	Substrate concentration (mg/L)	unstable		

	Biomass concentration (mg/L)			
Adaptive Backstepping	Substrate concentration (mg/L)	0.006	0.002	0.24
	Substrate concentration (mg/L)	1.37e-5	1.16e-4	0.01

5. CONCLUSIONS

In this paper, a new hybrid method is presented for control and regulation of MFC and by taking advantages of the adaptive method, chebyshev neural network approximator has been overcome to uncertainty, disturbance and nonlinear hard terms effects. The novel designed robust control method is a combination of sliding mode and output feedback techniques, which used to overcome the effects of noise and estimation error. Also, due to the use of hyperbolic functions in the proposed robust method, the control signals and the resulting states showed a smooth behavior. The simulation results showed that the proposed robust method is able to improve the transient and steady state response of system states in achieving control objectives and the desired power of the MFC output. Also, using the proposed controller, the stability of the system confirmed under the most severe operating conditions in terms of the presence of disturbance, parametric uncertainty and noise. Considering the limitations on the control signal as well as the controller optimization are the suitable ways to continue studies in this field.

ACKNOWLEDGMENT

This work was supported by the Science and Technology Development Plan Project of Jilin Province (Grant No. YDZJ202501ZYTS631).

REFERENCES

[1] Shahbaz, M., Raghutla, C., Chittedi, K. R., Jiao, Z., & Vo, X. V. (2020). The effect of renewable energy consumption on economic growth: Evidence from the renewable energy country attractive index. *Energy*, 207, 118162. <https://doi.org/10.1016/j.energy.2020.118162>

[2] Gozgor, G., Mahalik, M. K., Demir, E., & Padhan, H. (2020). The impact of economic globalization on renewable energy in the OECD countries. *Energy Policy*, 139, 111365. <https://doi.org/10.1016/j.enpol.2020.111365>

[3] Wang, W., Xie, R. K., & Ding, L. (2024). Stability analysis of load frequency control systems with electric vehicle considering time-varying delay. *IEEE Access*. <https://doi.org/10.1109/ACCESS.2024.3519343>

[4] Chen, X., Wei, S., Wang, J., Tong, F., Söhnel, T., Waterhouse, G. I., ... & Taylor, M. P. (2024). Lithium insertion/extraction mechanism in Mg₂Sn anode for lithium-ion batteries. *Intermetallics*, 169, 108306. <https://doi.org/10.1016/j.intermet.2024.108306>

[5] Cheng, T., Liu, Q., Jiang, G., Yang, B., Wang, X., & Wang, P. (2025). Numerical study of proton exchange membrane fuel cells with airfoil cross flow field. *Journal of Power Sources*, 631, 236232. <https://doi.org/10.1016/j.jpowsour.2025.236232>

- [6] Zhao, C., Song, Y., Chen, H., Chen, H., Li, Y., Lei, A., ... & Zhu, L. (2025). Improving the performance of microbial fuel cell stacks via capacitive-hydrogel bioanodes. *International Journal of Hydrogen Energy*, 97, 708-717. <https://doi.org/10.1016/j.ijhydene.2024.11.424>
- [7] Zhu, L., Song, Y., Chen, H., Wang, M., Liu, Z., Wei, X., ... & Ai, T. (2025). Optimization of power generation and sewage treatment in stacked pulsating gas-liquid-solid circulating fluidized bed microbial fuel cell using response surface methodology. *International Journal of Hydrogen Energy*, 101, 161-172. <https://doi.org/10.1016/j.ijhydene.2024.12.397>
- [8] Gajda, I., Greenman, J., & Ieropoulos, I. A. (2018). Recent advancements in real-world microbial fuel cell applications. *Current opinion in electrochemistry*, 11, 78-83. <https://doi.org/10.1016/j.coelec.2018.09.006>
- [9] Do, M. H., Ngo, H. H., Guo, W., Chang, S. W., Nguyen, D. D., Liu, Y., ... & Kumar, M. (2020). Microbial fuel cell-based biosensor for online monitoring wastewater quality: A critical review. *Science of The Total Environment*, 712, 135612. <https://doi.org/10.1016/j.scitotenv.2019.135612>
- [10] Estrada-Arriaga, E. B., Hernández-Romano, J., Mijaylova-Nacheva, P., Gutiérrez-Macías, T., & Morales-Morales, C. (2021). Assessment of a novel single-stage integrated dark fermentation-microbial fuel cell system coupled to proton-exchange membrane fuel cell to generate bio-hydrogen and recover electricity from wastewater. *Biomass and Bioenergy*, 147, 106016. <https://doi.org/10.1016/j.biombioe.2021.106016>
- [11] Yan, M., & Fan, L. (2013). Constant voltage output in two-chamber microbial fuel cell under fuzzy PID control. *Int. J. Electrochem. Sci*, 8, 3321-3332. [https://doi.org/10.1016/S1452-3981\(23\)14393-8](https://doi.org/10.1016/S1452-3981(23)14393-8)
- [12] Fu, L., Fu, X., & Imani Marrani, H. (2022). Finite Time Robust Controller Design for Microbial Fuel Cell in the Presence of Parametric Uncertainty. *Journal of Electrical Engineering & Technology*, 1-11. <https://doi.org/10.1007/s42835-021-00919-x>
- [13] Fan, L., Zhang, J., & Shi, X. (2015). Performance improvement of a microbial fuel cell based on model predictive control. *Int. J. Electrochem. Sci*, 10(1), 737-748. [https://doi.org/10.1016/S1452-3981\(23\)05028-9](https://doi.org/10.1016/S1452-3981(23)05028-9)
- [14] Patel, R., & Deb, D. (2019). Nonlinear adaptive control of microbial fuel cell with two species in a single chamber. *Journal of Power Sources*, 434, 226739. <https://doi.org/10.1016/j.jpowsour.2019.226739>
- [15] Patel, R., Deb, D., Dey, R., & Balas, V. E. (2020). Robust control design of SPSC microbial fuel cell with norm bounded uncertainty. In *Adaptive and Intelligent Control of Microbial Fuel Cells* (pp. 41-52). Springer, Cham. https://doi.org/10.1007/978-3-030-18068-3_4
- [16] Fu, X., Fu, L., & Marrani, H. I. (2020). A Novel adaptive sliding mode control of microbial fuel cell in the presence of uncertainty. *Journal of Electrical Engineering & Technology*, 15(6), 2769-2776. <https://doi.org/10.1007/s42835-020-00535-1>
- [17] Fu, X., Fu, L., Marrani, H. I., & Branch, A. Stabilization of A Single Chamber Single Population Microbial Fuel Cell by Using of a Novel Nonlinear Adaptive Sliding Mode Control Stabilization of A Single Chamber Single Population Microbial Fuel Cell by Using of a Novel Nonlinear Adaptive Sliding Mode Control. <https://doi.org/10.14447/jnmes.v24i1.a03>
- [18] Fu, L., Fu, X., & Imani Marrani, H. (2021). Robust adaptive fuzzy control for single-chamber single-population microbial fuel cell. *Systems Science & Control Engineering*, 9(1), 98-108. <https://doi.org/10.1080/21642583.2020.1870580>
- [19] Abul, A., Zhang, J., Steidl, R., Reguera, G., & Tan, X. (2016, July). Microbial fuel cells: Control-oriented modeling and experimental validation. In *2016 American Control Conference (ACC)* (pp. 412-417). IEEE. <https://doi.org/10.1109/ACC.2016.7524949>
- [20] Deolia, V. K., Purwar, S., & Sharma, T. N. (2012). Stabilization of unknown nonlinear discrete-time delay systems based on neural network. <http://dx.doi.org/10.4236/ica.2012.34039>
- [21] Hornik, K., Stinchcombe, M., & White, H. (1989). Multilayer feedforward networks are universal approximators. *Neural networks*, 2(5), 359-366. [https://doi.org/10.1016/0893-6080\(89\)90020-8](https://doi.org/10.1016/0893-6080(89)90020-8)
- [22] Yang, H., & Liu, J. (2018). An adaptive RBF neural network control method for a class of nonlinear systems. *IEEE/CAA Journal of Automatica Sinica*, 5(2), 457-462. <https://doi.org/10.1109/JAS.2017.7510820>
- [23] Polycarpou, M. M., & Ioannou, P. A. (1993, June). A robust adaptive nonlinear control design. In *1993 American control conference* (pp. 1365-1369). IEEE. <https://doi.org/10.23919/ACC.1993.4793094>
- [24] Patel, R., & Deb, D. (2018). Parametrized control-oriented mathematical model and adaptive backstepping control of a single chamber single population microbial fuel cell. *Journal of Power Sources*, 396, 599-605. <https://doi.org/10.1016/j.jpowsour.2018.06.064>